Multidisciplinary Design Approach for On-board High-speed Energy Conversion Machinery

Tuhin Choudhury
Dept. of Mechanical Eng.
LUT University
Lappeenranta, Finland
Tuhin.Choudhury@lut.fi

Juuso Narsakka
Dept. of Mechanical Eng.
LUT University
Lappeenranta, Finland
Juuso.Narsakka@lut.fi

Kristóf Márton Szombati
Dept. of Mechanical Eng.
LUT University
Lappeenranta, Finland
Kristof.Szombati@lut.fi

Sadjad Madanzadeh
Dept. of Electrical Eng.
LUT University
Lappeenranta, Finland
Sadjad.Madanzadeh@lut.fi

Valerii Abramenko
Dept. of Electrical Eng.
LUT University
Lappeenranta, Finland
Valerii.Abramenko@lut.fi

Niko Nevaranta
Dept. of Electrical Eng.
LUT University
Lappeenranta, Finland
Niko.Nevaranta@lut.fi

Henrik Ebel
Dept. of Mechanical Eng.
LUT University
Lappeenranta, Finland
Henrik.Ebel@lut.fi

Teemu-Turunen Saaresti
Dept. of Energy Tech.
LUT University
Lappeenranta, Finland
Teemu.Turunen-Saaresti@lut.fi

Juha Pyrhönen
Dept. of Electrical Eng.
LUT University
Lappeenranta, Finland
Juha.Pyrhonen@lut.fi

Jussi Sopanen
Dept. of Mechanical Eng.
LUT University
Lappeenranta, Finland
Jussi.Sopanen@lut.fi

***Abstract*—High-speed technology represents a transformative opportunity for advancing the energy transition in shipping, enabling more efficient and compact power generation solutions. This study proposes a rapid, multidisciplinary design approach for on-board high-speed electrical machines. It integrates process, rotordynamics, magnetic bearings, electromagnetic, and structural parameters, while accounting for ship motion effects. Traditional sequential design methods are comprehensive but time-consuming. Analytical design methods offer a faster alternative by iterating geometric parameters based on power and speed. However, existing methods often lack integration of structural and rotordynamics viewpoints with key performance aspects for marine applications, such as process, generator topology, and effects of ship motion. This study addresses these gaps using a high-pressure shaft system from a gas turbine on a marine vessel, highlighting the design compromises and interactions between dynamics and other areas of design.**

***Index Terms*—active magnetic bearings, high-speed technology, on-board machinery, multidisciplinary design.**

I. Introduction

The integration of high-speed (HS) electrical machines with active magnetic bearings (AMBs) is becoming one of the key technologies in the energy conversion sector due to the general trend towards increased efficiency and energy density. Typically, HS machines are designed using a systematic method that incorporates inputs from various disciplines such as electromagnetics, mechanical stress, thermal aspects, rotordynamics, control and manufacturability [1]. Each design aspect is addressed sequentially, and the design flow loops back to previous steps for marginal optimization where disciplines are correlated. A key shortcoming of this approach is that it is time-consuming and expensive as it requires customized design from scratch for each case [2]. An alternative approach for rapid design at conceptual stage is the Design Space Method (DSM). DSM uses analytical equations to rapidly iterate geometric parameters, generating possible values for each dimension based on power and speed requirements [3].

In recent years, with more focus in electrification of marine transportation [4], AMB supported HS machines have found new application as onboard energy conversion machines [5]. However, despite the extensive research on such systems as part of stationary units, the literature on their application as power generation unit aboard marine vessels is extremely limited.

For example, the DSM currently lacks integration with electromagnetic performance and process parameters, which are key factors when considering a megawatt-scale power generator unit for supplying electricity on a large marine vessel. Furthermore, ships are subjected to large motions due to maneuvering, propulsion and sea waves which generates additional forces acting on the rotor-AMB system due to gyroscopic effect and inertia. These forces acting in translational and rotational degrees of freedom (DOF) affect the dynamic behavior of the rotor-AMB system, often leading compromises in gas turbine efficiency and performance to achieve a feasible

This research was supported by the European Commission through the project 'Efficient Zero-Emissions Gas Turbine POWER System for MARitime Transport (MARPOWER)' and the Research Council of Finland's Centre of Excellence in High-Speed Energy Conversion Systems.

design. To the best of the authors knowledge, there are no studies that include these effect of large motions of moving platform in the initial, rapid design stage.

To that end, this study proposes a multidisciplinary design approach for onboard energy conversion machinery in a moving platform such as a marine vessel. The study extends the DSM to further include the electromagnetic and process parameters together with the structural and the rotordynamic aspects in the rapid design process. Furthermore, the study includes the gyroscopic effects and inertia from the large ship motions in the design process to study the compromises within the different disciplines. The study considers a high pressure (HP) shaft system from a gas turbine application on a marine vessel to analyze the results from this method. Fig. 1 shows a general example of an on-board, high-speed turbine - compressor - rotor machine.

II. Multi-disciplinary design for turbine - compressor - rotor system supported with AMBs

This section introduces the different aspects and design steps included in designing a turbine - compressor - rotor system for marine application. The thermodynamic cycle design provides the necessary inputs for the turbo-machinery components, as well as the electro-mechanical design of the HS machine.

A. Design inputs from process cycle and turbo-machinery

For turbo-machinery application, the most crucial parameter is the total efficiency of the thermodynamic process. This requires high temperatures, pressures and mass flow through the turbine combined with optimal compressor design. Based on these parameters, potential rotational speeds for the HS machine are listed, which is a key input for the rotor AMB system design. For this particular case, a generator output of 2.7 MW was selected and three different speeds: 13, 15, and 18 krpm were considered. The 15 krpm speed was selected as a compromise between efficiency and feasibility, especially considering 15% over-speed requirement for the turbines in marine application.

Another key design input from process cycle are the forces from the fluid flow. To attain negligible radial forces from the process cycle, an axial turbine is chosen here along with two stages centrifugal compressors. The net axial force, influenced by turbine and compressor configurations, is another key input to conceptual design. The compressors and turbines are placed opposite to each other to partially balance the axial forces. For multi-stage compressors, the impellers can be arranged in series or back-to-back configuration [6]. With compressors HPC1 and HPC2 in series, the net axial forces are 4500 N at design point operation, and 13300 N in emergency shutdown situation. The turbine and compressor geometries, which are modeled as mass points further affect the overall dynamics of the rotor AMB system. Table I shows a list of the inputs from the process cycle and turbomachinery components.

B. Generator topology

The next step in the design process is to select the topology and dimensions for the active part of the rotor. At surface velocities close to 200 m/s, there are two potential topologies; permanent magnet (PM) synchronous motor rotor, and induction motor (IM) with a solid rotor topology. This part of the design and comparison needs to be carried out using FEM iterations between electrical design, mechanical design and generator cooling.

In order to achieve a good balance between performance and cooling, a slitted rotor with copper squirrel cage configuration was selected for the IM. For the PM machine, the magnets were segmented and placed in an aluminum cage, supported by supported by a carbon fiber sleeve. In both cases, air flow from external fans achived the necessary cooling by dissipating the generated heat through cooling channels. The stator is liquid cooled to achieve the desired current density and dissipate the generated heat. Table II provides the necessary dimensions and parameters for both topologies.

C. Mechanical stresses

For feasibility analysis, the stresses in various rotating components can be evaluated using analytical equations [7]. The radial and tangential stresses for solid rotor shaft and for laminates such as AMB actuators, spacers, sensors, end rings, and sleeves due to centrifugal forces can estimated at radius r_r as:

$$\sigma_\mathrm{r} = \frac{3+\nu_\mathrm{d}}{8}\rho_\mathrm{d}\Omega^2(r_\mathrm{in}^2 + r_\mathrm{out}^2 - \frac{r_\mathrm{in}^2 r_\mathrm{out}^2}{r_\mathrm{r}^2} - r_\mathrm{r}^2), \quad (1)$$

$$\sigma_\theta = \frac{3+\nu_\mathrm{d}}{8}\rho_\mathrm{d}\Omega^2(r_\mathrm{in}^2 + r_\mathrm{out}^2 + \frac{r_\mathrm{in}^2 r_\mathrm{out}^2}{r_\mathrm{r}^2} - \frac{1+3\nu_\mathrm{d}}{3+\nu_\mathrm{d}}r_\mathrm{r}^2), \quad (2)$$

where ν_d is the Poisson's ratio, ρ_d is the material density, Ω is the rotational speed, r_in is the disk inner radius and r_out outer radius.

Table I: Inputs from the process cycle and turbomachinery components

Parameters	Value
Process parameters	
Power (Electrical) (MW)	2.70
Nominal Speed (rpm)	15 000
Over-speed (rpm)	18 000
Turbomachinery components	
High-pressure compressor stage 1 (HPC1)	
Axial length (mm)	148.00
Outlet diameter (mm)	469.68
Hub diameter (mm)	22.00
Mass (kg)	18.26
Polar moment of Inertia (kg·m^2)	0.30
Diametral moment of Inertia (kg·m^2)	0.18
High-pressure compressor stage 2 (HPC2)	
Axial length (mm)	85.00
Outlet diameter (mm)	473.40
Hub diameter (mm)	80.00
Mass (kg)	15.25
Polar moment of Inertia (kg·m^2)	0.31
Diametral moment of Inertia (kg·m^2)	0.16
High-pressure turbine (HPT)	
Axial length (mm)	188.00
Mean diameter (mm)	583.70
Mass (kg)	108.16
Polar moment of Inertia (kg·m^2)	4.60
Diametral moment of Inertia (kg·m^2)	2.30

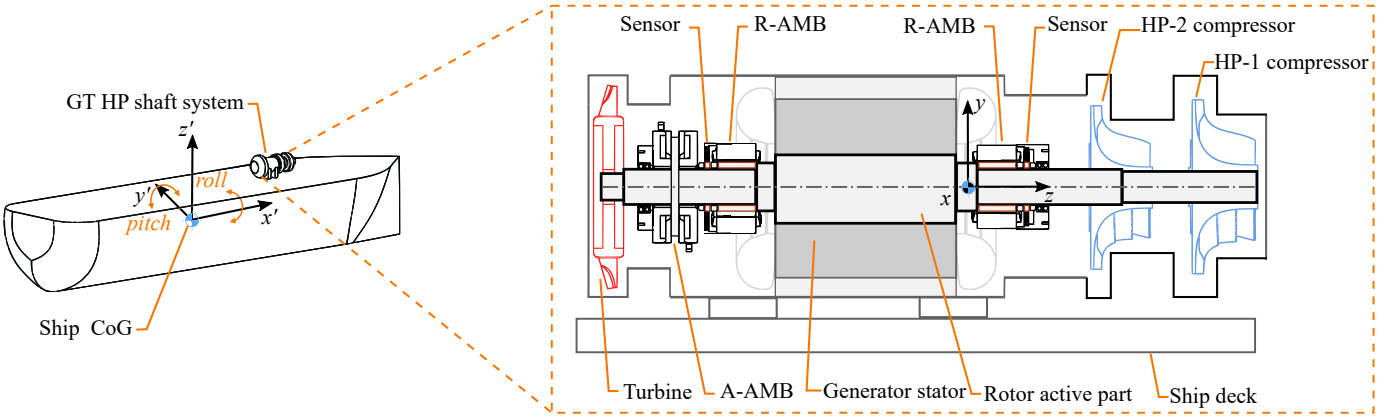

Figure 1: Example of an onboard, high-speed energy conversion machinery as part of power generation unit in a marine vessel. The key components which are determined from various disciplines are also highlighted in the figure.

Table II: Main parameters of the 2700 kW 15000 pmn IM and PM generator

Parameters	IM	PMSM
Axial length	563	410
Outer stator diameter	641	590
Rotor diameter	237	242
Power (MW)	2.7	2.7
Speed (rpm)	14 969	15 000
Pole pair number	1	2
Fundamental supply frequency (Hz)	250	500
Torque (Nm)	1 725.3	1 744
Rated phase current RMS (A)	1 564.5	3362
Current density (A/mm2)	10.86	11.4
Line-to-Line voltage (V)	660	665.6
Stator winding Joule losses (W)	15 315	15331
Stator Iron losses (W)	6 502	12332
Rotor Joule losses (W)	10 174	2433
Air gap friction (W)	3 572*	2000*
Total losses (W)	35 563	33 298
Efficiency (%)	98.7	98.84
Power factor	0.813	0.706

* Analytically estimated

The maximum stress, $\sigma_{\max}$, can be calculated with

$$\sigma_{\max} = \frac{1}{4} \cdot \rho_{\mathrm{d}} \cdot \Omega^2 \cdot \left((1-v) \cdot r_{\mathrm{in}}^2 + (v+3) \cdot r_{\mathrm{out}}^2\right) \quad (3)$$

The stresses in active part requires special considerations. For the slitted rotor squirrel cage design in IM, a comprehensive method for calculating the stresses analytically was presented and verified in our previous study [8]. The most critical part in IM designs are end rings [2], [9]. After initial feasibility check, finite element analysis (FEA) should be performed to ensure proper contact between the bars and end ring assembly.

For the PM topology, the stresses can be estimated roughly including effects of interference and thermal expansion using analytical equations (with 15 % safety margin). Detailed FEA is required to validate the values, especially for the interaction between the rotor, the aluminum cage, the magnets, and the carbon fiber sleeve an the resulting stresses [10].

D. Rotordynamic model

1) Shaft model: The finite element method (FEM) is used for constructing the rotor model. The rotor shaft is discretized into several three-dimensional beam elements along its axis of rotation, following Timoshenko's beam theory [11]. Each node of the rotor has two translational and two rotational - degrees of freedom for lateral vibration analysis. The model takes the geometry and physical properties of the rotor as input.

The equation of motion for the rotor can be described in general terms as,

$$\mathbf{M}\ddot{\mathbf{q}} + (\mathbf{D} + \Omega\mathbf{G})\dot{\mathbf{q}} + \mathbf{K}\mathbf{q} = \mathbf{F}, \quad (4)$$

where $\mathbf{M}$ is the mass matrix, $\mathbf{D}$ is the damping matrix, Ω is the rotational speed, $\mathbf{G}$ is the groscopic matrix and $\mathbf{K}$ is the stiffness matrix of the system. $\mathbf{F}$ is the force vector including unbalance force $\mathbf{F}_{\mathrm{u}}$ and gravitational force $\mathbf{F}_{\mathrm{g}}$. $\mathbf{q}$, $\dot{\mathbf{q}}$ and $\ddot{\mathbf{q}}$ represent the displacement, velocity and acceleration vectors, respectively.

Equation (4) can be represented in state-equation form by substituting $\mathbf{q}_1 = \mathbf{q}$ and $\mathbf{q}_2 = \dot{\mathbf{q}}$ [12], resulting in

$$\begin{cases} \dot{\mathbf{q}}_1 = \dot{\mathbf{q}} = \mathbf{q}_2, \\ \dot{\mathbf{q}}_2 = \ddot{\mathbf{q}} = -\mathbf{M}^{-1}(\mathbf{F} - (\mathbf{D} + \Omega\mathbf{G})\mathbf{q}_2 - \mathbf{K}\mathbf{q}_1). \end{cases} \quad (5)$$

Thus in the state-space form, (4) can be written as:

$$\begin{bmatrix} \dot{\mathbf{q}}_1 \\ \dot{\mathbf{q}}_2 \end{bmatrix} = \begin{bmatrix} \mathbf{0} & \mathbf{I} \\ -\mathbf{M}^{-1}\mathbf{K} & -\mathbf{M}^{-1}(\mathbf{D} + \Omega\mathbf{G}) \end{bmatrix} \begin{bmatrix} \mathbf{q}_1 \\ \mathbf{q}_2 \end{bmatrix} + \begin{bmatrix} \mathbf{0} \\ \mathbf{M}^{-1}\mathbf{F} \end{bmatrix}, \quad (6)$$

where $\mathbf{I}$ is the identity matrix.The state matrix of (6), denoted by $\mathbf{A}$, can be used to solve the eigenvalue problem as:

$$\mathbf{A}\mathbf{v} = \lambda\mathbf{v}, \quad (7)$$

with $\mathbf{v} \neq 0$, the eigenvalues will appear in the form of complex conjugate pairs

$$\lambda_i = \alpha_i \pm j\beta_i, \quad (8)$$

where, α_i and β_i represent the real and imaginary parts respectively and $j = \sqrt{-1}$. The damped natural frequencies Ω_i and the damping ratios ζ_i for i^{th} mode can be written as

$$\Omega_i = \sqrt{{\alpha_i}^2 + {\beta_i}^2}, \tag{9}$$

$$\zeta_i = -\frac{\alpha_i}{\sqrt{\alpha_i^2 + \beta_i^2}}. \tag{10}$$

2) AMB model: The linearized AMB model includes the bearing current stiffness and position stiffness together with the mechanical (FEM) model of the rotor in the state space form (6). For example the linearized forces can be given as

$$\mathbf{F}_{\text{AMB}} = -\mathbf{K}_q \mathbf{q}_a + \mathbf{K}_i \mathbf{i}_a, \tag{11}$$

where, $\mathbf{q}_\text{a}$ and $\mathbf{i}_\text{a}$ are the displacements at AMB locations and control currents respectively. The current stiffness $\mathbf{K}_\text{i}$ and position stiffness $\mathbf{K}_\text{q}$ are defined at the operating point ($q = 0$, $i_\text{a} = 0$) where the analytical expressions are generalized assuming no saturation and no fringing flux paths.

$$\mathbf{K}_\text{i} = \frac{\mu_0 N^2 A_{\text{pole}} i_\text{b}}{l_0^2}, \mathbf{K}_\text{q} = \frac{\mu_0 N^2 A_{\text{pole}} i_\text{b}^2}{l_0^3}, \tag{12}$$

where A_{pole} is the pole area, N is the number of turns, l_0 is mean airgap, i_b is the bias current, and μ_0 is permeability of air. The linearized plant models are used for the control synthesis.

3) Overall equation of motion: The overall equation of motion for the rotor-AMB system can be expressed as:

$$\mathbf{M}\ddot{\mathbf{q}} + (\mathbf{D} + \Omega\mathbf{G})\dot{\mathbf{q}} + \mathbf{K}\mathbf{q} = \mathbf{F}_\text{u} + \mathbf{F}_\text{g} - \mathbf{F}_{\text{AMB}}. \tag{13}$$

Including the AMB support conditions using a PD controller, the state matrix can be represented as

$$\mathbf{A}_1 = \begin{bmatrix} \mathbf{0} & \mathbf{I} \\ -\mathbf{M}^{-1}(\mathbf{K} + \mathbf{K}_\text{P}\mathbf{K}_\text{i} - \mathbf{K}_\text{q}) & -\mathbf{M}^{-1}(\mathbf{D} + \mathbf{K}_\text{D}\mathbf{K}_\text{i} + \Omega\mathbf{G}) \end{bmatrix}, \tag{14}$$

where $\mathbf{K}_\text{P}$ and $\mathbf{K}_\text{D}$, are the proportional and derivative gains respectively. The Campbell diagram can be computed by calculating rotation speed Ω dependent values, such as gyroscopic matrix, for each spin speed and then performing an eigenvalue solution for that speed with equations (7)–(10).

E. Bearing configurations

The design inputs from turbomachinery and rotor topology are used as an input to create a preliminary sketch of the rotor shaft. Based on the rotor layout, potential bearing locations are identified. For each bearing configuration, a rotordynamic analysis is performed for the rotor-AMB system using extended DSM. In our previous study presenting DSM [3], the HS machine was studied with a single IM configuration and AMB configuration. For the current rotor layout, five different configurations – representing radial and axial active magnetic bearings, (denoted as R-AMB and A-AMB) – are investigated in this study (Fig. 2). Rotor dynamics are evaluated with beam element model, where turbine and compressors are modeled as point masses.

Table III: Maximum allowable inclination in ships (Length ≥ 100 m) applied to onboard gas turbines [13]

Rotational motion		Angle of inclination [°]	
		Static	Dynamic (Time period [s])
Fore-and-aft (Pitch)		5	7.5 (5)
Athwartship (Roll)		15	25 (10)

F. Ship motion modeling

As Fig. 1 shows, in ship motion analysis, the x_{ship}-axis runs longitudinally from bow to stern, the y_{ship}-axis extends laterally from port to starboard, and the z_{ship}-axis is vertical from hull to deck. Translational motions along these axes include surge (x_{ship}), sway (y_{ship}), and heave (z_{ship}), while rotational motions include roll (around x_{ship}), pitch (around y_{ship}), and yaw (around z_{ship}).

However, as per international standards and class requirements [13], ensuring the machinery performs under pitch and roll motion is sufficient. Addressing the maximum pitch and roll movements (Table III) is expected to provide the necessary damping for the other movements.

For this step, the rotor bearing configuration needs to be established already. The mass of all the rotating components along with the location of the turbine on the ship, and its orientation will contribute to the forces due to ship motion. The additional bearing force considering only the pitch and roll motions of the vessel can be expressed as

$$\mathbf{F}_{\text{bm}} = \mathbf{m}\left(\dot{\boldsymbol{\omega}} \times \mathbf{r} + \boldsymbol{\omega} \times (\boldsymbol{\omega} \times \mathbf{r})\right) + \frac{\mathbf{I}_\text{d}\dot{\boldsymbol{\omega}} + \mathbf{I}_\text{p}\left(\Omega + \beta\right)\dot{\alpha}}{\mathbf{a} + \mathbf{b}} \tag{15}$$

where m is the mass of the rotor, $\boldsymbol{\omega}$ is the angular velocity vector of the vessel base motion, $\mathbf{r}$ is the position vector of the center of inertia (CoI) of the rotor expressed in the frame of reference of the vessel, $\mathbf{I}_\text{d}$ and $\mathbf{I}_\text{p}$ are the diametral and polar mass moment of inertia of the rotor, α and β are the angle of pitch and roll of the vessel and a and b are the turbine and compressor side R-AMB distances measured from the CoI of the rotor.

III. Analysis of different rotor configurations

In order to narrow down the design options, first the initial parameters are established for the thermodynamic process, the turbomachinery, and the generator topologies. The next steps are related to the rotordynamics, mechanical design, stress calculations, ease of assembly and taking into account the forces due to operation on a marine vessel.

A. Baseline Rotordynamics (Pre-analysis)

A baseline model is created for the rotor-AMB system using the DSM in all possible configuration and a pre-check is carried out by evaluating the rotordynamics. Note that the rotor topology (PM or IM) does not play a significant part

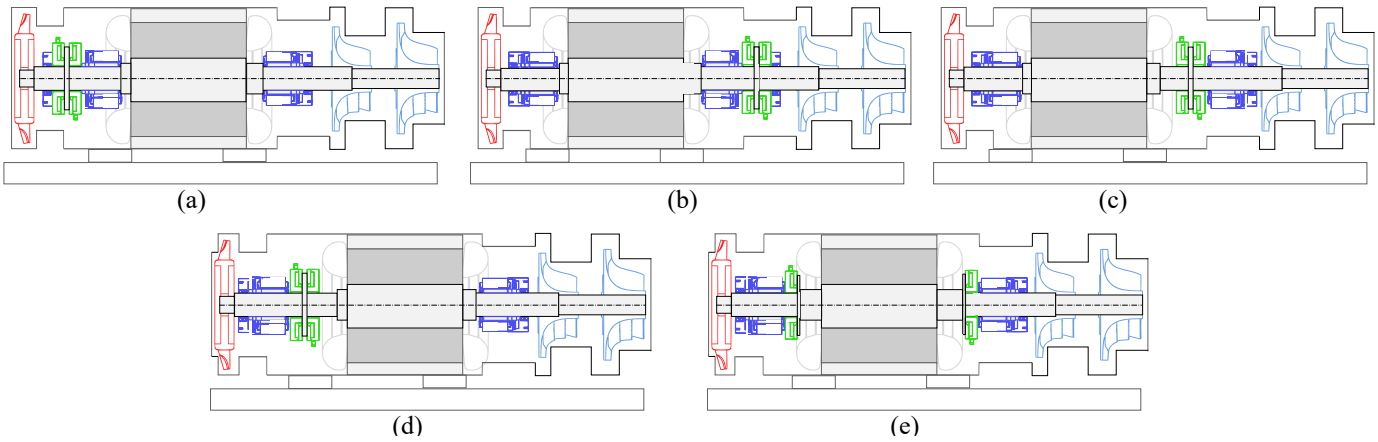

Figure 2: (a)–(e) Five different bearing configurations (D1–D5) developed for initial assessment. The green components represent the A-AMB while the blue components represent the R-AMBs.

Table IV: Critical speeds (in rpms) for different bearing configurations. The highlight shows proximity to operational speed of 15 000 rpm (darker shade means the particular critical speed is closer to the operational speed).

Bearing configs	1st BW	1st FW	2nd BW	2nd FW	1st Tor	2nd Tor
D1	5800	7000	9400	14800	12400	17400
D2	5400	6600	9200	15200	11840	18200
D3	6600	8000	10000	16800	13400	18200
D4	6600	8000	10200	16600	13400	18000
D5	6600	7800	10000	16200	13200	17800

at this stage, and the goal is to simply establish the rough critical speeds, operational limitations and mode shapes using the nominal speed and electrical power as inputs.

In this study, the baseline rotor configurations were created for 15 000 rpm and 2.7 MW output power. Table IV presents the critical speeds for D1 to D5 design configurations, which correspond to the five different bearing layouts. The results indicate that an under critical rotor system cannot be achieved for this setup, as the 1st FW critical speed is about 6600–8000 rpms for all configurations. More importantly, the data further shows that the 2nd FW critical speed is close to the operational speed of 15 000 rpm for all cases. As a result, the rotor dynamics became a key challenge and required more investigation with established bearing and generator topology for this case study.

B. Mechanical stresses and design considerations

Before proceeding to a second iteration of rotordynamics with more detailed rotor model, the mechanical stresses of the generator components can be checked to ensure both IM and PM options are feasible. The maximum stress in IM 237 designs were found to be 410 MPa at 15 000 rpm, occurring at the end ring region. This implies that the end ring and the conductive bar assembly should be optimized as the strength values for end ring material (typically made of highly conductive copper alloys) are in the range of 350-450 MPa. It should be also noted that modifying the end ring geometry, along with some safety margin, might increase the length of the rotor, which should be taken into account in the 2nd iteration of rotordynamic analysis.

For the PM242 designs, the stresses at the magnetic diameter of the rotor are around 1100 MPa at overspeed with 6 mm thickness in sleeve. While carbon fibre composites are available with material strength of up to 1800 MPa, some safety margin is required due to zero yield capacity of carbon fibre. In summary, both rotor topologies should be doable from the point of view of mechanical stresses, and should be considered for the next iteration of rotordynamics.

From the initial five cases of AMB configurations, the options can be further narrowed down based on ease of manufacturing, assembly, and cooling possibilities. For example, while D5 (Fig. 2 (e)) might be advantageous in terms of manufacturability and cost, it leaves minimal space for introducing cooling flow in the air gap. Similarly, both D3 and D4 are feasible designs, but the axial AMB in those configurations is not fully utilized to manage the thermal expansion of the shaft and precise axial positioning of the compressor or turbine impellers. This leaves us with the more conventional designs D1 (Fig. 2 (a)) and D2 (Fig. 2 (b)). Despite the rotordynamic challenges in the baseline estimates (Table IV), these designs offer several advantages such as convenience of assembly, better rotor cooling option, and improved controllability of turbine or compressor processes. To keep this study concise, the option D1 is chosen for second round of rotordynamic iteration with detailed generator and AMB component design.

C. Rotordynamic analyses and bearing configurations

Table V shows the critical speed analysis results from the second iteration of rotordynamics. The PM vs IM comparison indicates that the D1 PM242 configuration is the best potential rotor topology, as at 15 000 rpm nominal speed, it can operate very well between the 1st and 2nd forward modes with sufficient safety margins from both. Fig.3 shows preliminary rotordynamics of the selected configuration.

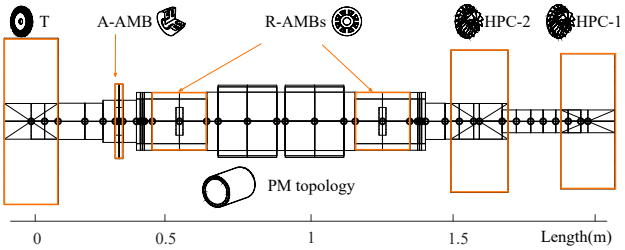

(a) FEM model of D1 PM242 rotor

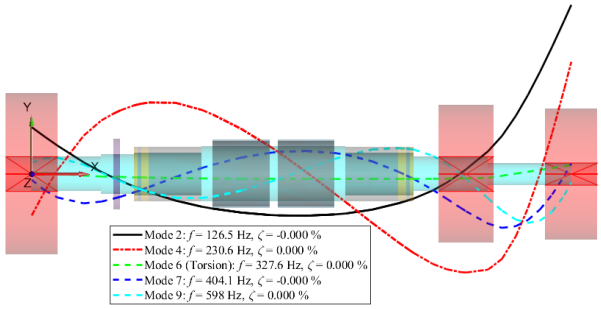

(b) First three bending modes (free-free)

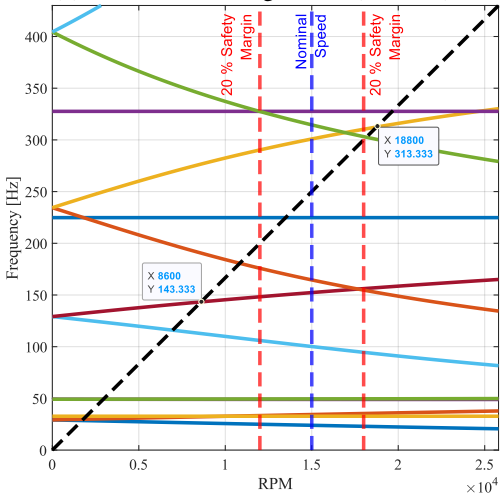

(c) Campbell diagram: critical speeds and operational range for AMB supported rotor

Figure 3: (a) A FEM model, (b) mode shapes and natural frequencies and (c) a Campbell diagram of the selected design: D1 PM 242.

D. Sensitivity study

In the final stages of conceptual design, it is essential to investigate the sensitivity of key parameters within the overall design to anticipate how the dynamic behavior of the rotor-AMB system will respond to any potential changes in the future. Fig. 4 shows the sensitivity analyses for D1 PM242 design. Two parameters were selected for analysis; Compressor mass properties were varied within ± 20%, and the load factor (LF) for radial magnetic bearings were varied from 4 to 7. The results show that the LF has a huge impact on the 2nd critical speed and hence can be considered for tuning that mode if needed.

Table V: Critical speeds for IM and PM topologies for D1 bearing configurations

	1st BW	1st FW	2nd BW	2nd FW	1st Tor	2nd Tor
D1 IM237	5200	6400	8800	13800	11400	17400
D1 PM242	7000	8600	10800	18800	13600	19800

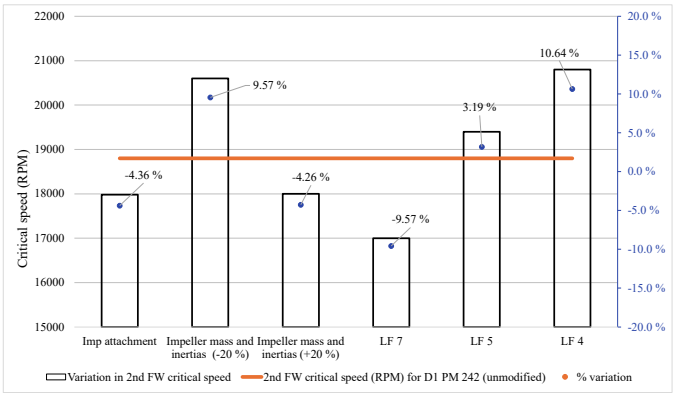

Figure 4: Sensitivity study of different factors affecting the 2nd FW critical speed.

E. Integration of ship motion

The selelcted rotor D1PM242 had a mass of 576.4 kg and the coordinates of the CoI of the shaft system, expressed in the frame of reference of the vessel, are (-50 m, 14 m, and 25m) in x', y' and z' direction respectively. α is the pitch angle and β is the roll angle of the ship.

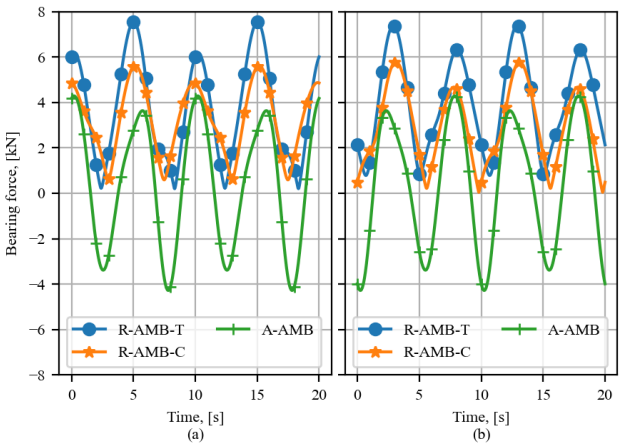

Figure 5: Bearing forces considering (a) 0° and (b) 180° phase between ship pitch and roll motions. R-AMB-T denotes the turbine-side, R-AMB-C denotes the compressor-side bearing.

Fig. 5 presents the forces acting in the radial and axial directions induced by the pitch and roll motions of the ship. For the D1 PM 242 rotor considered here, the maximum radial and axial force amplitudes due to ship motions are approx. 7500 N and 4300 N respectively. Therefore, the radial

and especially, the axial AMBs should be designed with enough force capacity to handle these loads without reaching magnetic saturation or exceeding the current and voltage limits of the amplifier. The raidal and axial AMB considered in this paper are designed to have a total maximum capacity of 15 kN, defined by the process-related forces and operational constraints to ensure stable performance of the conceptual turbine-compressor, where the dimensions of an AMBs were optimized through an analytical optimization process. As a result the design D1PM242 should work very well for the intended onboard application. With this, the iterative initial feasibility check is now complete, and the study progresses next to the detailed design phase.

IV. Conclusion

This study proposes a step-by-step design methodology for rapid, multidisciplinary design of an onboard HS electrical machines. The method considers the thermodynamic cycle, turbomachinery, AMB configurations, preanalysis of rotordyanmics, mechanical stresses in rotor, AMB and generator topologies and the consecutive rotordynamic behavior to identify the best option from perspectives. Furthermore, a sensitivity study is carried out to analyze how changing certain key variables affect the rotordynamics of the system to evaluate the limitations of the design. Lastly, when the effect of key ship motions on the rotor-AMB system is analyzed to evaluate if the load capacity of the AMBs are sufficient.

The proposed method is suitable for evaluating the feasibility of several options, and narrowing down the choices at the conceptual design stage of an onboard HS machine. After this point, more detailed design work can proceed within individual disciplines, reducing inter-dependencies and iterations that could otherwise cause delays and hinder the product development and commissioning timeline.

References

[1] A. Grönman, J. Nerg, E. Sikanen, T. Sillanpää, N. Nevaranta, E. Scherman, A. Uusitalo, N. Uzhegov, A. Smirnov, J. Honkatukia *et al.*, "Design and verification of a hermetic high-speed turbogenerator concept for biomass and waste heat recovery applications," *Energy Conversion and Management*, vol. 225, p. 113427, 2020.

[2] J. Narsakka, T. Choudhury, J. Sopanen, J. Pyrhönen, and J. Nerg, "High-speed induction-machine squirrel-cage rotor mechanical design evaluation," in *2024 International Conference on Electrical Machines (ICEM)*. IEEE, 2024, pp. 1–8.

[3] E. Kurvinen, T. Choudhury, J. Narsakka, I. Martikainen, J. Sopanen, and R. P. Jastrzebski, "Design space method for conceptual design exploration of high speed slitted solid induction motor," in *2021 IEEE International Electric Machines & Drives Conference (IEMDC)*, 2021, pp. 1–8.

[4] M. Tadros, M. Ventura, and C. Guedes Soares, "Review of the imo initiatives for ship energy efficiency and their implications," *Journal of Marine Science and Application*, vol. 22, no. 4, pp. 662–680, 2023.

[5] T. Soni, J. K. Dutt, and A. S. Das, "Magnetic bearings for marine rotor systems—effect of standard ship maneuver," *IEEE Transactions on Industrial Electronics*, vol. 68, no. 2, pp. 1055–1064, 2021.

[6] X. Qiu, J. Hua, C. Qian, J. Wang, W. Xuan, B. Yu, J. Shi, and J. Chen, "Experimental study on system characteristics of vapor compression refrigeration system using small-scale, gas-bearing, oil-free centrifugal compressor," *Energy*, vol. 307, p. 132690, 2024.

[7] E. Kurvinen, T. Choudhury, J. Narsakka, I. Martikainen, J. Sopanen, and R. P. Jastrzebski, "Design space method for conceptual design exploration of high speed slitted solid induction motor," in *2021 IEEE International Electric Machines & Drives Conference (IEMDC)*, 2021.

[8] J. Narsakka, K. Vostrov, T. Choudhury, E. Kurvinen, J. Sopanen, and J. Pyrhönen, "Method for mechanical design of squirrel cage slitted solid rotor," in *2022 International Conference on Electrical Machines (ICEM)*. IEEE, 2022, pp. 2135–2141.

[9] M. Caprio, V. Lelos, J. Herbst, and J. Upshaw, "Advanced induction motor endring design features for high speed applications," in *IEEE International Conference on Electric Machines and Drives, 2005.* IEEE, 2005, pp. 993–998.

[10] A. Borisavljevic, *Limits, modeling and design of high-speed permanent magnet machines*. Springer Science & Business Media, 2012.

[11] H. Nelson, "A finite rotating shaft element using timoshenko beam theory," *J Mech Des*, vol. 102, no. 4, pp. 793–803, 1980.

[12] D. J. Inman, *Engineering vibration. Pearson*. Pearson Education, 2014.

[13] ClassNK, "Unified requirements for machinery installations," August 2024, rev. 4. [Online]. Available: https://www.classnk.or.jp/hp/pdf/info_service/iacs_ur_and_ui/ur-m46-rev.4-aug-2024-ul.pdf